

Multi-modal Microscopy Characterisation of Nodal Markings in Flax Fibre

Hongjia Zhang, Tan Sui, Lisbeth G. Thygesen, Patrick O'Brien, and Alexander M. Korsunsky*

Abstract—Natural fibres such as kenaf, sisal, flax etc. have gained increasing recognition as alternatives to hi-tech synthetic fibres, primarily due to their moderate cost and environmentally friendly nature. However, the well-reported wide variability of their properties, primarily stiffness and strength, presents a significant challenge to the use of these fibres in composite materials and systems that have important implications for reliability and safety. Understanding the sources of variability requires combining different methods of structural analysis, as it is done in the context of multi-modal microscopy reported here. The morphology and internal architecture of flax nodal markings (sometimes also called “dislocations”) are described, and their implications for strength discussed.

Index Terms— flax fibre; nodal markings; polarized optical microscopy; FIB-SEM; microstructure

I. INTRODUCTION

FLAX fibres are being used as a substitute for synthetic glass fibres reinforcement in polymer matrix composite, due to their high performance mechanical properties and environmental and ecological benefits. However, it has been found that flax fibres also contain defects known as nodal markings, slip lines or dislocations that in some studies have been found to be related to their strength [1]. In fact, the body of evident relating the tensile strength of individual fibres to dislocation is contradictory [2-5]. Dislocations appear to provide the location for crack initiation [6-8] and therefore are included in the strength models of single fibres as regions

Manuscript received April 08, 2015; revised April 09, 2015.

(This work was supported in part by EU FP7project iSTRESS “Pre-standardisation of incremental FIB micro-milling for intrinsic stress evaluation at the sub-micron scale”, and by EPSRC through grants EP/I020691 “Multi-disciplinary Centre for In-situ Processing Studies (CIPS)”, EP/G004676 “Micromechanical Modelling and Experimentation”, and EP/H003215 “New Dimensions of Engineering Science at Large Facilities”).

Hongjia Zhang is doctoral student in the Department of Engineering Science, University of Oxford, OX1 3PJ, UK (e-mail: hongjia.zhang@eng.ox.ac.uk).

Tan Sui is postdoctoral research assistant in the Department of Engineering Science, University of Oxford, OX1 3PJ, UK (e-mail: tan.sui@eng.ox.ac.uk).

Lisbeth G. Thygesen is Senior Researcher University of Copenhagen, Institut for Geovidenskab og Naturforvaltning, Skov, natur og biomasse, Rolighedsvej 23, Frederiksberg C Denmark 1958, Denmark (e-mail: lgt@ign.ku.dk)

Patrick O'Brien is Senior International Environmental Consultant, Toll Environmental Consulting Limited, 23 Lower Woodlands, Kerry Pike, Co. Cork, Ireland (e-mail: ptobien18@gmail.com).

*Alexander M. Korsunsky is Professor of Engineering Science at the University of Oxford, OX1 3PJ, UK (corresponding author, tel: +44-18652-73043; fax: +44-18652-73010; e-mail: alexander.korsunsky@eng.ox.ac.uk).

of reduced strength [9, 10]. The investigation of the microstructure of nodal markings at micro- and nano-scale level may give better insight into the relationships between structure and mechanical properties, as well as other aspects of fibre behavior, e.g. functional properties. Focused Ion Beam – Scanning Electron Microscope (FIB-SEM) serial sectioning has been successfully applied in order to visualize the way in which individual flax fibres are assembled into bundles, and also to image the structure of the secondary wall of a single fibre [11]. The proven feasibility of utilizing FIB-SEM to characterize the inner structure of natural flax fibres leads us to pursue further our attempt to carry out closer and more detailed observation on the nodal markings found in natural flax fibres. The precise identification of the region of interest (ROI) was achieved with the help of polarized light microscopy (PLM). This was followed by FIB sectioning and high resolution SEM imaging of selected local regions to reveal denser pore distribution inside the nodal markings than the surrounding region. It is hypothesized that it is this increased presence of internal voids in the nodal markings regions that play a role for the strength properties of natural fibres and result in failure being located at the nodal markings sites.

II. METHODS

A. Sample Preparation

The flax fibres studied in this experiment were isolated from unbleached flax fibre bundles (*Linum usitatissimum* L.) purchased from the company Skytten. A bunch of fibres was separated from a fibre stem and soaked in water for a while. Under a long focal distance digital microscope, the fibres were separated from the bunch by hand using tweezers.

Isolated fibres with the length of approximately 1.5 mm were mounted on a glass plate for the use in an optical microscope to locate the nodal markings. One of the challenges of multi-modal imaging was to identify and implement a sample mounting arrangement that allowed interchangeability between optical transmission imaging through a glass slide (transmission mode), on the one hand, and FIB-SEM imaging in the vacuum chamber of the electron microscope (reflection mode), on the other. The two microscopy techniques are highly complementary, in terms of resolution (fractions of a micron optically vs a few nm in the SEM), image formation (full field optically vs scanning mode in the SEM), structural sensitivity (polarization of transmitted light sensitive to the orientation of cellulose polymer molecule carbon backbone direction vs surface topography contrast in SEM), and beam path (transmission through the entire fibre optically vs very near-surface

information in secondary electrons (SE) or backscattered electrons (BSE) in SEM). Nevertheless, it was hoped that the prominent and distinct structural features of nodal markings would allow registration, i.e. alignment, to be achieved between moderate resolution optical imaging and high resolution electron and ion microscopy.

To this end, the sample still mounted on the glass slide used for optical transmission imaging was placed on an aluminium alloy SEM stub, and charge path was provided with silver paint applied at each end. To reduce the charging effect in SEM, the sample was coated with a Au-Pd layer to the thickness of a few nanometres using the mini sputter coater (SC7620, Quorum Technologies).

B. Polarized Light Microscopy (PLM)

Olympus BX51 optical microscope was utilized for fibre imaging with transmitted light. A 360-degree adjustable polarizer was placed in the light path to impose a linear polarization on the illumination coming from the back lighting source. The interaction of the linearly polarized incident light with the sample induced partial polarization from different parts of the fibre. It has already been well-established that the light polarization induced by the nodal markings is different from the rest of the fibre [12,13]. Transmitted light was then passed through another polarizing plate (analyser). The imaging contrast of the nodal markings was achieved by first adjusting the analyser angular position to ensure cross polarization between the two plates; and then rotation both plates together with respect to the fibre. This procedure ensured that nodal markings became prominently visible as bright features, whilst the rest of the fibre appeared darker. A digital camera attached to the microscope was used to collect a sequence of images to form a mosaic covering the entire length of the fibre, from one end to the other, with some overlap between images for alignment.

Gimp (version 1.2) was the software used for image processing to obtain the complete composite mapping image of the fibre of the kind illustrated in Fig. 2a.

C. FIB-SEM Serial Sectioning

LYRA3 (Tescan s.r.o, Brno, Czech Republic) was utilized for FIB-SEM serial sectioning experiment. Electron beam used for SEM imaging had the voltage of 5.0 kV and emission current of 189.3 μ A. The ion beam used for milling had the voltage of 30.0 kV and the current of 53 pA. Fig. 1 gives a schematic illustration of the FIB-SEM configuration used in this study. Focused Ion Beam was directed from the top and was incident normally on the top surface of material. Using moderate to high ion current resulted in material removal (“milling”) from material surface inwards. The electron beam column is mounted at a fixed offset angle of 55° from the vertical FIB column, meaning that the surface was imaged at an oblique angle of 35°. Correction for the imaging distortion induced by this oblique angle could be provided in two ways: by changing the scanning parameters to ensure that the electron probe was rastered over an rectangular array on the sample surface such that the steps in the two in-plane directions were equal; or in the software mode, i.e. simply by stretching the image along the “short” direction after the data was collected. The former approach was used, since it

provided higher quality imaging data, and also allowed the use of dynamic focusing that took into account the varying distance made from the electron objective lens to different points on the sample surface due to oblique incidence.

TABLE I
PARAMETERS FOR SEM-FIB SERIAL SECTIONING

Parameter		Value
Milling volume	width	21.77 μ m
	depth	15 μ m
	length	4.15 μ m
Slices	thickness	25 nm
	number of SEM images	166
SEM image	pixel size	25 \times 25 nm ²
	matrix size of Image frame	1220 \times 949

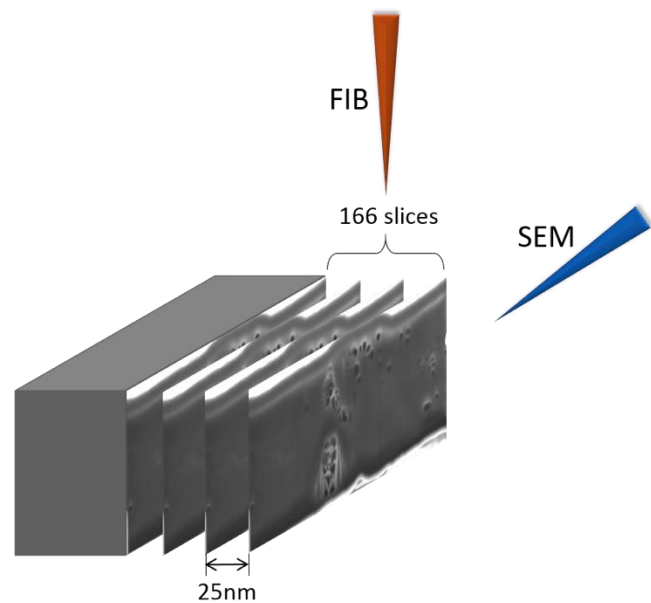


Fig. 1. Schematic demonstration of FIB-SEM configuration in a FIB-SEM serial sectioning experiment conducted on a nodal marking of flax fibres

An important consideration in the preparation of FIB-SEM serial sectioning experiment is maintaining the convergence of the electron and ion beams, to ensure that SEM images are collected from the precise location where ion beam milling is performed. The intersection between the two beams was carefully aligned, enabling stable centre of SEM images and avoiding image drift. Layers of material with thickness of 25 nm were removed in sequence by FIB at the current of 53 pA. Each newly exposed surface was translated by the same 25nm to place the new surface in the same position as in the previous step, and the next image was acquired by the SEM. The milling width was set to be 21.77 μ m and the depth to 15 μ m. This was to make sure that at each milling step covered the complete cross-section of the chosen flax fibre. The milling length was set to be 4.15 μ m, meaning that 166 slices were removed, and 167 images collected in total. To study the internal structure of a dislocation, adequate resolution for SEM images were required. Therefore, the pixel size was set to 25 \times 25 nm², and the matrix size of 1220 \times 949 pixels was used for each image. Table 1 gives a summary of the parameters used for FIB-SEM serial sectioning of flax fibres

in this study.

III. RESULTS

Figure 2b illustrates the sample mounting arrangement, with the two silver paint dots used to immobilize the fibres, and also served as reference to localize the nodal markings by evaluating the distance along the fibre. S_1 and S_2 labels denote the silver paint dots, with red dash lines indicating the boundaries in Fig. 2a. The distance from the chosen dislocation (highlighted by the red dashed rectangle) to the edge (designated by "M") of silver paint dot in the area of S_1 was measured as $a=577.6\mu\text{m}$ approximately along the longitudinal direction of flax fibre.

Polarized light microscopy image of two flax fibres is shown in Fig. 2a. The nodal markings displayed as bright bands appear systematically along each individual flax fibre. It is clear that in order to achieve detailed observation of these features with the characteristic dimensions of $10\text{-}20\mu\text{m}$, high resolution imaging method at the nanoscale is needed in order to visualize their structure.

A higher magnification of PLM image is shown in Fig. 3 on the left, with the dislocation / nodal marking ROI again marked by the red dash rectangle. The two steps were used to identify nodal marking of interest from the full mapping of Fig. 2a:

- i) differentiate the two ends of fibre according to the shape of silver paint;
- ii) measure the distance between the chosen dislocation and a certain end.

After the sample was carefully transferred to the electron microscope chamber, SEM acquisition was used in order to locate the correct nodal markings for further observations. Point M was firstly identified under lower magnification and then the sample was translated towards the chosen dislocation by $577.6\mu\text{m}$ using accurate sample stage control, leading exactly to the region of interest. Under the magnification matched to that of the PLM image in Fig.3, the SEM image shown on the right hand side of Fig.3 was collected. Those large enough nodal markings are quite clearly visible at the fibre surfaces, since these dislocations are defined not only as irregular regions within the cell wall, but also as topographic contrast at the fibre side surfaces, as discussed earlier [14]. Clear confirmation of alignment can be seen by comparing the PLM and SEM images in Fig. 3. Thus, the ROI was identified correctly, and further multi-scale insight into the internal architecture of a nodal marking can be obtained by FIB-SEM serial sectioning.

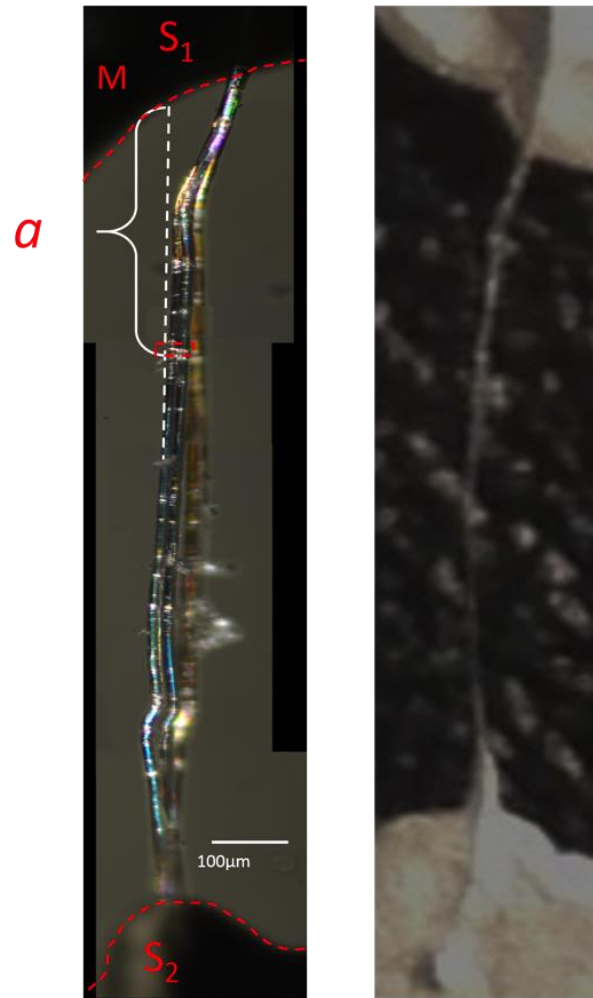


Fig. 2. a) Full mapping of the fibre using crossed plates PLM illustrating the presence of nodal markings. The region of interest (ROI) used for FIB-SEM serial sectioning is highlighted as the red rectangle. b) Illustration of sample mounting on a glass substrate using conductive silver paint.

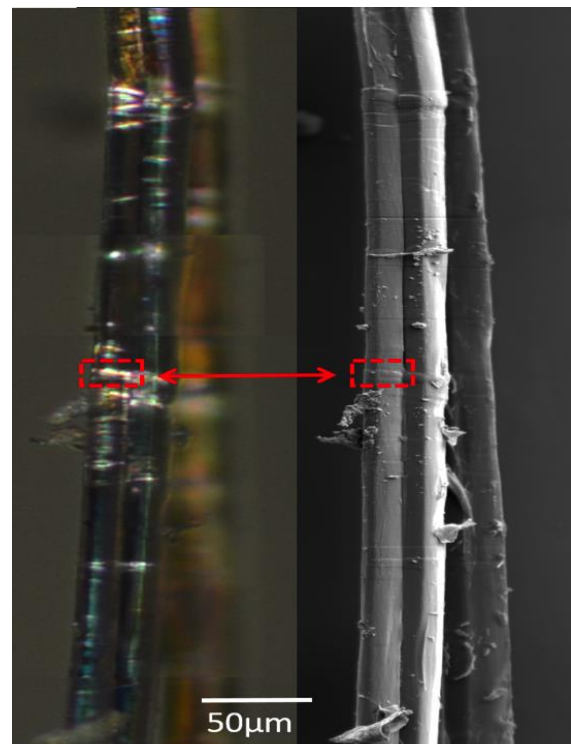


Fig. 3. ROI location in the SEM and comparison between dislocation image from SEM and fibre mapping image from cross-polarized light microscopy.

In order to allow the discussion of the internal structure of a nodal marking, a representative cross-section SEM image is shown in Figure 4. This image was selected from a series of FIB-SEM sectioning snapshots to illustrate the internal arrangement within a nodal marking that reveals several aspects of the effect it is likely to have on the structural integrity (strength) of the fibre. It is worth noting that the topography relief observed on the external surface of the fibre is associated with a cluster of internal voids located just sub-surface, and leading to a degree of “bulging” of the exterior fibre wall. Furthermore, it can be noticed also that significant defects and pores are present in the bulk of the fibre at the location proximate to the nodal marking. They are located close to the centre of the image, and have the internal diameter of the order of one micron. Such large pores are not evenly distributed along the fibre length: it is evident that the pores are clustered in the vicinity of the nodal marking, although some are visible at a moderate distance from it.

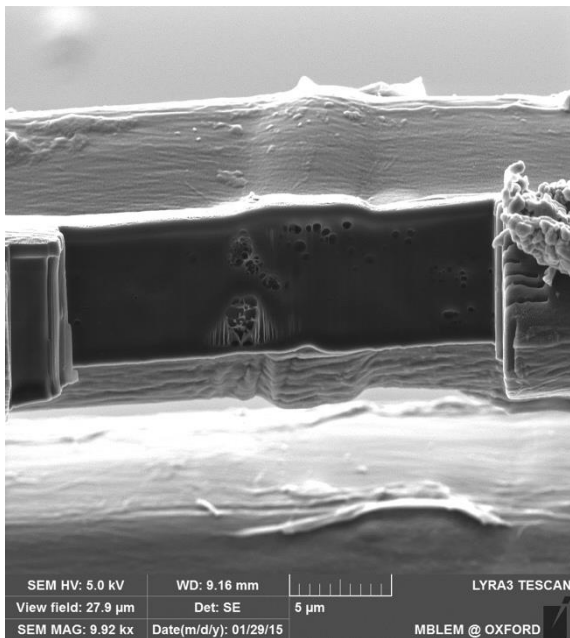


Fig. 4. A snapshot selected from the FIB-SEM serial sectioning sequence showing the characteristic features and inner microstructure of a nodal marking.

Figure 5 is presented here to illustrate the kind of information that can be derived from sequential FIB-SEM serial sectioning. As the observed section progresses across the nodal marking that was chosen for examination, the principal void is seen to reveal internal structuring consisting of multiple internal voids separated by thin membranes, forming a “bubble cluster” with the effective size of a few microns. The presence of such void results in a significant reduction in the load-bearing cross-sectional area, and therefore may be expected to serve as the “weakest link” in a long fibre subjected to a tensile load. This is in line with the observations reported previously using synchrotron X-ray diffraction [15], which revealed the presence of micron-sized clusters of voids in the form of a sizeable cavity around the fibre lumen found periodically along the fibre length.

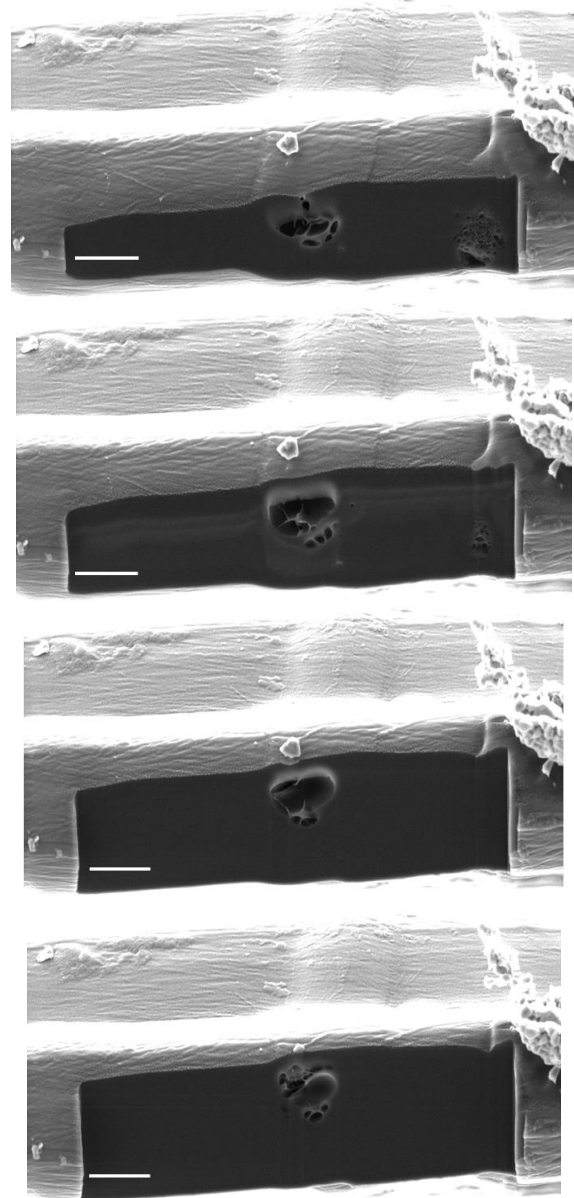


Fig. 5. A sequence of images from FIB-SEM serial sectioning showing the depth variation and progress of inside the nodal marking: a) 58th image (depth=1.45 µm) b) 90th image (depth=2.25 µm) c) 120th image (depth=3.0 µm) d) 147th image (depth=3.675 µm). Scale bar = 2.5 µm

IV. DISCUSSION AND CONCLUSION

The combination of polarized light microscopy (PLM) and Scanning Electron Microscopy (SEM) with Focused Ion Beam (FIB) enables multi-modal microscopy examination of natural flax fibres for the purpose of accurate identification of nodal markings. This signifies an important step towards nano-scale inner structural visualization of these interesting natural structures.

The presence of inner porous microstructure at nodal markings represents defects that might lead to the failure. Considering the inconsistency nodal markings introduce to the inner structure, fibres are weakened and more likely to fail at dislocations under loading. Since nodal markings are a natural and integral feature of flax fibres, a possible way to reduce their affect would be to seek a fibre species that is less susceptible to nodal marking formation, that responds to the variation in the growing conditions to reduce the nodal

marking formation, or may even perhaps allow genetic modification to create a species that is free from such defects. However, as nodal markings possibly have vital stress dissipation functions in the living plant these ideas remain entirely speculative.

Complementary techniques e.g. EDX and EBSD that as part of the common SEM configuration will be applied in the future to provide multi-modal characterization of the similar objects. Further experimental and modelling investigations of the correlation between the structure of nodal markings and fibre strength distribution will be carried out.

2010). August 1-6, 2010 (Singapore), IFMBE Proceedings Volume 31, 2010, pp. 1151-1154.

ACKNOWLEDGMENT

The authors express their gratitude to Zora Strelcova and Jiri Dluhos at TESCAN Brno, s.r.o., Czech Republic, for their ongoing advice and support in the operation of FIB-SEM facilities in the Multi-Beam Laboratory for Engineering Microscopy (MBLEM), Department of Engineering Science, University of Oxford, UK.

REFERENCES

- [1] L. G. Thygesen, N. Gierlinger (2013) *The molecular structure within dislocations in Cannabis sativa fibres studied by polarised Raman microspectroscopy*, Journal of Structural Biology, vol. 182, pp. 219-225.
- [2] C. Baley (2004) *Influence of kink bands on the tensile strength of flax fibers*, Journal of Materials Science, vol. 39, pp. 331-334.
- [3] G.C. Davies, D. M. Bruce (1998) *Effect of environmental relative humidity and damage on the tensile properties of flax and nettle fibers*, Textile Research Journal, vol. 68, pp. 623-629.
- [4] M. Eder, N. Terziev, G. Daniel, et al (2008) *The effect of (induced) dislocations on the tensile properties of individual Norway spruce fibres*, Holzforschung, vol. 62, pp. 77-81.
- [5] A. Thygesen, A. B. Thomsen, G. Daniel, et al (2007) *Comparison of composites made from fungal defibrated hemp with composites of traditional hemp yarn*, Industrial Crops and Products, vol. 25, pp. 147-159.
- [6] C. Baley (2002) *Analysis of the flax fibres tensile behaviour and analysis of the tensile stiffness increase*, Composites Part A: Applied Science and Manufacturing, vol. 33, pp. 939-948.
- [7] O. L. Forgacs (1961) *Structural weaknesses in softwood pulp tracheids*, Tappi, vol. 44, pp. 112-119.
- [8] D. H. Page, F. El-Hosseiny, K. Winkler, et al (1972) *The mechanical properties of single wood-pulp fibres. Part I: A new approach*, Pulp and Paper Magazine of Canada, vol. 73, pp. 72-77.
- [9] J. Andersons, E. Poriķe, E. Spārniņš (2011) *Modeling strength scatter of elementary flax fibers: The effect of mechanical damage and geometrical characteristics*, Composites Part A: Applied Science and Manufacturing, vol. 42, pp. 543-549.
- [10] M. Aslan, G. Chinga-Carrasco, B. F. Sørensen, et al (2011) *Strength variability of single flax fibres*, Journal of materials science, vol. 46, pp. 6344-6354.
- [11] T. Sui, H. Zhang, S. Ying, P. O'Brien, A. M. Korsunsky, *FIB-SEM serial sectioning nanotomography of flax fibres*. Proceedings of the International Multi-Conference of Engineers and Computer Scientists (IMECS 2015), Hong Kong, March 2015.
- [12] L.G. Thygesen, P. Hoffmeyer (2005) *Image analysis for the quantification of dislocations in hemp fibres*, Industrial Crops and Products, vol.21, pp.173-184.
- [13] L.G. Thygesen (2010) *Dislocations in plant fibres and in Turin shroud fibres*, International Workshop on the Scientific approach to the Acheiropoietos Images, pp. 63-66.
- [14] L. G. Thygesen, J. B. Bilde-Sørensen, P. Hoffmeyer (2006) *Visualisation of dislocations in hemp fibres: A comparison between scanning electron microscopy (SEM) and polarized light microscopy (PLM)*, Industrial Crops and Products, vol. 24, pp. 181-185.
- [15] B. Abbey, S. Eve, A. Thuault, K. Charlet, A.M. Korsunsky (2010) *Synchrotron X-Ray tomographic investigation of internal structure of individual flax fibres*, 6th World Congress of Biomechanics (WCB